Supporting Information for

Synthesis-structure-function relationships of silica-supported niobium(V) catalysts for alkene epoxidation with H_2O_2

*Nicholas E. Thornburg, Scott L. Nauert, Anthony B. Thompson, Justin M. Notestein**

Department of Chemical and Biological Engineering, Northwestern University,
2145 Sheridan Road, Technological Institute E136, Evanston, IL 60208, USA

* j-notestein@northwestern.edu
847.491.5357 (phone)
847.491.3728 (fax)

Contents

Materials Synthesis

Grafted catalysts from Nb-calix[4]arene ("Cx") precursor. 3.7 mmol $NbCl_5$ was added to a 40 mL toluene suspension of 3.7 mmol p-*tert*-butylcalix[4]arene inside of an Ar glovebox. The flask was equipped with a magnetic stirbar, sealed, transferred to a Schlenk line under N_2 and affixed with a reflux condenser. The contents were refluxed for 14 h with continuous sparging of N_2; extent of reaction was monitored with pH strips placed at the vent. The suspension was cooled to 90°C, and discrete 10 mL volumes were syringe-transferred to three flasks containing variable amounts of partially-dehydroxylated SiO_2 under N_2 purge. The contents were refluxed for 24 h, after which the solids were vacuum-filtered in air, washed with anhydrous toluene and dried under dynamic vacuum (<30 mTorr) for >24 hours. Dried materials were calcined in air at 550°C for 6 h at a ramp rate of 10°C min^{-1} immediately before use.

Grafted catalysts from other Nb precursors (Cl, Cp, OEt, DMA). 0.60 mmol Nb precursor (~0.2 mmol Nb g^{-1} final "low-loaded" catalysts) or 1.87 mmol Nb precursor (~1.5 mmol Nb g^{-1} final "high-loaded" catalysts) were dissolved in anhydrous, degasified toluene inside of an Ar glovebox. Reaction flasks were equipped with a magnetic stirbar, sealed and transferred to a Schlenk line under N_2 purge. After attaching a condenser, contents were refluxed for 3 h before air-free addition of partially-dehydroxylated SiO_2 (3 g for low-loaded, 1 g for high-loaded). The suspension was refluxed for an additional 24 h, after which solids were vacuum-filtered in air, washed with anhydrous toluene, and dried under dynamic vacuum (<30 mTorr) overnight. Dried catalysts were air-calcined at 550°C for 6 h at a ramp rate of 10°C min^{-1} before subsequent use.

For $NbCl_5$ only, an identical procedure to the one above was followed for quantitatively grafting the precursor to SiO_2 to give final loadings of 0.070, 0.095, 0.140, 0.486 and 0.921 mmol Nb g^{-1} in the calcined materials. See Figure 3 and Table 1 in the main text. Further, we note that Nb-0.97-OEt has 0.97 mmol Nb g^{-1} as the highest grafting density achieved from a single cycle.

Nb-SBA-15 materials. Catalysts Nb-0.XX-SBA-15 (0.XX = 0.08, 0.10 mmol Nb g^{-1}) followed a slightly modified literature procedure.[1-2] 4.0 g of Pluronic P-123 triblock copolymer (Sigma, average M_n ~ 5800) was weighed out in a 250 mL round-bottom flask. 130 mL 18 MΩ·cm H_2O and 20 mL concentrated HCl (Macron, 37 wt%) were added simultaneously, and the suspension was stirred 16 h at ambient conditions for complete dissolution of the polymer. After simultaneous addition of 40.7 mmol tetraethyl orthosilicate ("TEOS," Sigma, 98%) and a discrete amount of niobium(V) oxalate hydrate (Alfa): 0.89 mmol Nb for Si:Nb = 50, and 0.39 mmol Nb for Si:Nb = 120. The contents were heated to 55°C with stirring for 8 h. Then, stirring was ceased, and the suspension was heated to 80°C for an additional 16 h. After cooling, the solids were recovered by vacuum-filtration, washed with 500 mL 18 MΩ·cm H_2O, and dried under dynamic vacuum (<30 mTorr). Final solids were calcined in air at 550°C for 6 h at a ramp of 10°C min^{-1} before subsequent use. SBA-15 structures were confirmed with low-angle pXRD (Figure S2) and N_2 physisorption (Figure S3).

Impregnated Nb-SiO_2 materials. Catalysts Nb-0.XX-Ox-IWI (0.XX = 0.21, 0.54 mmol Nb g^{-1}) were synthesized by incipient wetness impregnation of partially-dehydroxylated SiO_2 support (BET pore volume 0.95 cm^3 g^{-1}) at ambient conditions. 0.62 mmol or 1.54 mmol Nb(V) oxalate hydrate were dissolved in 2.85 mL 18 MΩ·cm H_2O and added dropwise to two beakers containing 3.0 g SiO_2, while continually dispersing the moist solids with a glass stir rod. (The more concentrated precursor solution was found to be the practical solubility limit.) Impregnated solids were dried at ambient conditions for 14 h, and then under dynamic vacuum (<30 mTorr) for 12 h. The dried materials were air-calcined at 550°C for 6 h at a ramp rate of 10°C min^{-1} before use as catalysts.

Group 4, 5 grafted catalysts. Synthesis of metallocalix[4]arene complexes of Ti(IV), Zr(IV), Hf(IV), Nb(V) and Ta(V) and of the subsequent SiO_2-grafted catalysts Ti-0.22-mmCx, Zr-0.23-dmCx, Hf-0.22-dmCx, Nb-0.20-Cx, and Ta-0.19-Cx are detailed in a previous report by some of us.[3] Control materials M-0.XX-Cl (M = Ti, Zr, Hf, Nb, Ta; 0.XX ~ 0.20 mmol M g^{-1}) are synthesized here following a similar procedure: 0.63 mmol MCl_x precursor were weighed out in a glovebox under Ar atmosphere, transferred to a 50 mL roundbottom flask equipped with a magnetic stirrer, and dissolved in 20 mL of dry, degasified toluene. Flasks were sealed, transferred from the glovebox to a Schlenk line under N_2 purge, fitted with a reflux condenser and heated to reflux for 3 h. The solution was then cooled to 90°C for the air-free addition of 3 g partially-dehydroxylated SiO_2. The suspension was refluxed for 24 h, cooled and vacuum-filtered in air. Solids were washed with 100 mL anhydrous toluene and dried under dynamic vacuum (<30 mTorr) overnight. Dried solids were calcined at 550°C for 6 h in air at a ramp rate of 10°C min^{-1} immediately before catalytic use.

Kinetic Discussion and Fitting. Kinetics assume fully-equilibrated binding of water and H_2O_2, as shown in Scheme 2 (reproduced below with speciation labels "B," "C" and "D" for clarity and additional constants labeled):

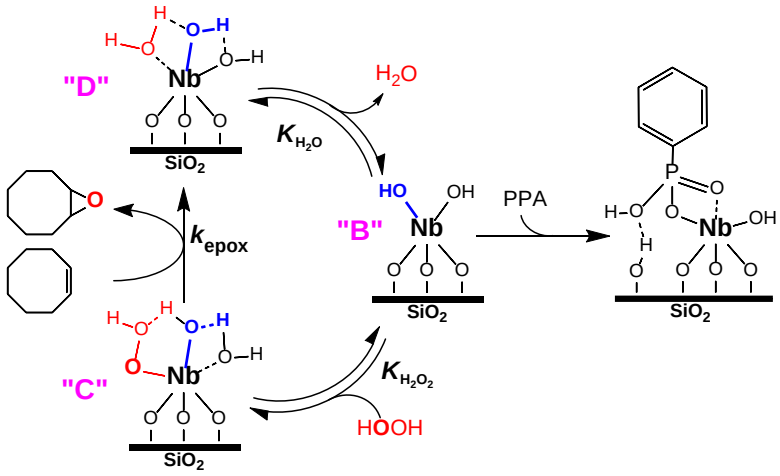

Scheme 2 (from main text). Proposed catalytic cycle for alkene epoxidation by H_2O_2 over highly dispersed Nb-SiO_2 with *in situ* titration with PPA. Scheme reproduced from main text with additional speciation labels and constants added for clarity.

In brief, [**B**] is the population of resting Nb-dihydroxy species, [**C**] is the population of Nb-hydroperoxo species, and [**D**] is the population of water-bound Nb species, which are also the product of peroxygen transfer in the epoxidation step. Assuming these species to be equilibrated, their interconversion can also be written in a manner analogous to the discussion in the main text:

$$\mathbf{B} + H_2O_2 \overset{K_{H2O2}}{\longleftrightarrow} \mathbf{C} \quad \textbf{or} \quad 2(NbOH) + H_2O_2 \overset{K_{H2O2}}{\longleftrightarrow} NbOH + NbOOH \cdot H_2O \tag{1}$$

$$\mathbf{B} + H_2O \overset{K_{H_2O}}{\longleftrightarrow} \mathbf{D} \quad \textbf{or} \quad 2(NbOH) + H_2O \overset{K_{H_2O}}{\longleftrightarrow} NbOH + NbOH \cdot H_2O \tag{2}$$

The rate limiting step of the reaction is proposed to be the transfer of the peroxygen to cyclooctene to directly give the epoxide product, which is catalyzed by an adjacent NbOH:

$$\mathbf{C} + \text{alkene} \overset{k_{epox}}{\longrightarrow} \mathbf{D} \quad \textbf{or} \quad NbOH + NbOOH \cdot H_2O + \text{alkene} \overset{k_{epox}}{\longrightarrow} NbOH + NbOH \cdot H_2O \tag{3}$$

This leads to an initial rate expression analogous to that in the main text:

$$r_0 = k_{epox}[NbOH][NbOOH \cdot H_2O][alkene]_0 \tag{4}$$

Using the equilibrium of (1), the rate expression is rewritten as:

$$r_0 = k_{epox}K_{H_2O_2}[NbOH]^2[H_2O_2]_0[alkene]_0 \tag{5}$$

A site balance on all active Nb ligands, written as $NbOH_{active}$, gives

$$[NbOH_{active}] = [NbOH] + [NbOH \cdot H_2O] + [NbOOH \cdot H_2O] \tag{6}$$

Applying the equilibrium relationships of (1) and (2), one gets:

$$[NbOH_{active}] = [NbOH]\left(1 + K_{H_2O}[H_2O] + K_{H_2O_2}[H_2O_2]\right) \tag{7}$$

Giving a rate expression of

$$r_0 = \frac{k_{epox}K_{H_2O_2}[NbOH_{active}]^2[H_2O_2]_0[alkene]_0}{\left(1+K_{H_2O}[H_2O]_0+K_{H_2O_2}[H_2O_2]_0\right)^2} \tag{8}$$

Recalling the irreversible titration of all active NbOH groups by PPA, and the introduction of the term $\boldsymbol{A}$ to account for the fraction of active Nb, we define $NbOH_{active}$ as in the main text:

$$[NbOH_{active}] = [NbOH_{total}] * \boldsymbol{A} - [PPA] \quad (9)$$

Inserting (9) into the rate expression (8) and defining the apparent rate constant k_{app} as the product $k_{epox}*K_{H2O2}$, we express the initial rate of epoxide production as:

$$r_0 = \frac{k_{app}([NbOH_{total}]*\boldsymbol{A}-[PPA])^2[H_2O_2]_0[alkene]_0}{\left(1+K_{H_2O}[H_2O]_0+K_{H_2O_2}[H_2O_2]_0\right)^2} \quad (10)$$

Initial rates of epoxide production were determined from control experiments with varying water and sub-stoichiometric PPA concentrations for Nb-0.20-Cx, and the data were fit to Eq. 10 using MATLAB R2010b software an iterative generalized least-squares regression to determine equilibrium constants K_{H2O} and K_{H2O2}.

All following fits were insensitive to the product $K_{H2O2}*[H_2O_2]$, indicating its magnitude was $\ll 1$, and for all future discussion this term has been removed from the denominator. The fitted value of K_{H2O} was 0.77 M^{-1} and was taken as constant for all other Nb-SiO_2 catalysts for subsequent modeling. Eq. 11 shows the slightly simplified overall initial rate model:

$$r_0 = \frac{k_{app}([NbOH_{total}]*\boldsymbol{A}-[PPA])^2[H_2O_2]_0[alkene]_0}{\left(1+K_{\mathrm{H_2O}}[H_2O]_0\right)^2} \quad (11)$$

This kinetic model is not intended to be definitive, but it is able to capture the supralinear response to added titrant while also compensating for small differences in the amount of H_2O present. Catalysts Nb-0.07-Cl, Nb-0.10-Cl, and Nb-0.14-Cl were excluded from fitting due to insufficient data (very low rates) at sub-stoichiometric additions of PPA. Initial rates from the remaining 18 Nb-SiO_2 catalysts at sub-stoichiometric charges of titrant were then fit to determine independent parameters k_{app} and A for each catalyst. Accordingly, k_{app} as calculated here represents the rate constant for active catalytic species and does not capture the ~5% residual activity observed at higher charges of PPA (e.g. Figure 6b). We further note that since k_{app} is the product $k_{epox}*K_{H2O2}$, the model is unable to decouple values of k_{epox} and K_{H2O2}. All values are given in Table S3.

Finally, we note that competing H_2O_2 decomposition was not included in the model, since the total concentration of H_2O_2 does not substantially decrease in the first minutes of reaction over which the initial rates were computed (Figure S7, Table S5). Further, the H_2O_2 decomposition rates over these two catalysts are both ~1.7x their respective epoxidation rates, suggesting that the same type of active site participates in both epoxidation and unproductive H_2O_2 decomposition.

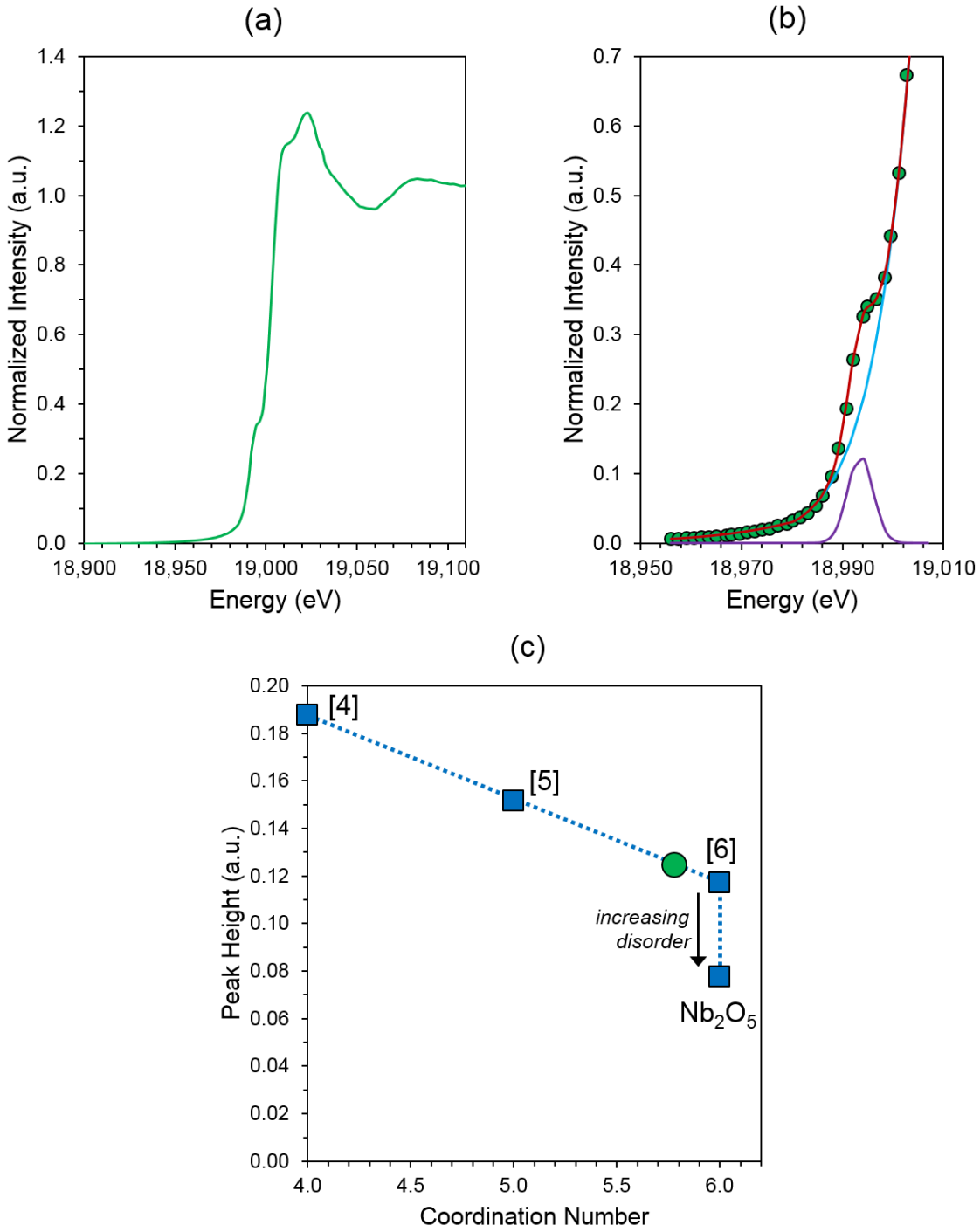

Figure S1. Representative Nb *K*-edge XANES for Nb-0.23-Cp: (a) normalized spectrum; (b) peak fitting of pre-edge feature; and (c) linear correlation between pre-edge feature height and standards of known coordination (blue squares), then used to interpolate coordination number of Nb-0.23-Cp (green circle). Data points in (c) enlarged to illustrate error of fitting technique. Dashed line represents trend. See Table S1. All materials are dried for analysis.

Table S1. Nb *K*-edge XANES summary for standards and calcined Nb(V)-silica catalysts.

		Pre-edge[b]		
Material	**E_0[a] (eV)**	**Energy (eV)**	**Intensity**	**C.N.[b]**
$YNbO_4$	18,992	18,994	0.19	[4]
$CaNb_2O_6$	18,992	18,993	0.15	[5][c]
$KNbO_3$	18,992	18,994	0.12	[6]
Nb_2O_5	18,993	18,993	0.08	[6][d]
Nb-0.07-Cx	18,992	[e]	[e]	[e]
Nb-0.10-Cx	18,992	18,993	0.17	4.4
Nb-0.13-Cx	18,992	18,993	0.18	4.3
Nb-0.20-Cx	18,992	18,993	0.17	4.5
Nb-0.07-Cl	18,992	[e]	[e]	[e]
Nb-0.10-Cl	18,992	18,993	0.12	5.8
Nb-0.15-Cl	18,992	18,993	0.14	5.5
Nb-0.20-Cl	18,992	18,993	0.13	5.7
Nb-0.49-Cl	18,992	18,993	0.11	6.0
Nb-0.92-Cl	18,993	18,994	0.13	5.6
Nb-1.53-Cl	18,992	18,994	0.12	5.9
Nb-0.23-Cp	18,992	18,994	0.12	5.8
Nb-1.61-Cp	18,992	18,993	0.12	6.0
Nb-0.21-DMA	18,992	18,993	0.14	5.4
Nb-1.57-DMA	18,992	18,994	0.12	5.8
Nb-0.20-OEt	18,992	18,994	0.13	5.6
Nb-0.97-OEt	18,993	18,994	0.12	6.0
Nb-0.08-SBA-15	18,992	[e]	[e]	[e]
Nb-0.10-SBA-15	18,992	[e]	[e]	[e]
Nb-0.21-Ox-IWI	18,992	18,994	0.15	5.1
Nb-0.54-Ox-IWI	18,992	18,994	0.12	5.8

[a] Computed from position of zero-crossing of the second derivative.
[b] See Figure S1 above for fitting technique.[3]
[c] The structure is effectively 5-coordinate since one bond in the Nb octahedron is very long (2.342 Å).[4-5]
[d] Disordered 6-coordinate structure.
[e] Pre-edge feature and C.N. not determined due to low signal-to-noise in spectra (attributed to low Nb content).

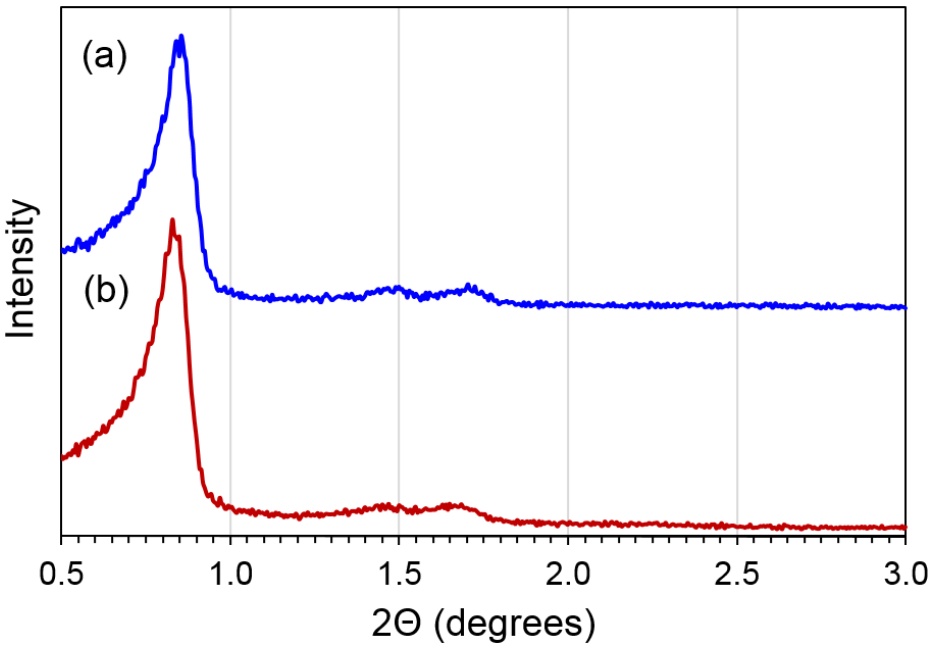

Figure S2. Low-angle powder x-ray diffraction (pXRD) patterns for catalysts (a) Nb-0.08-SBA-15 and (b) Nb-0.10-SBA-15.

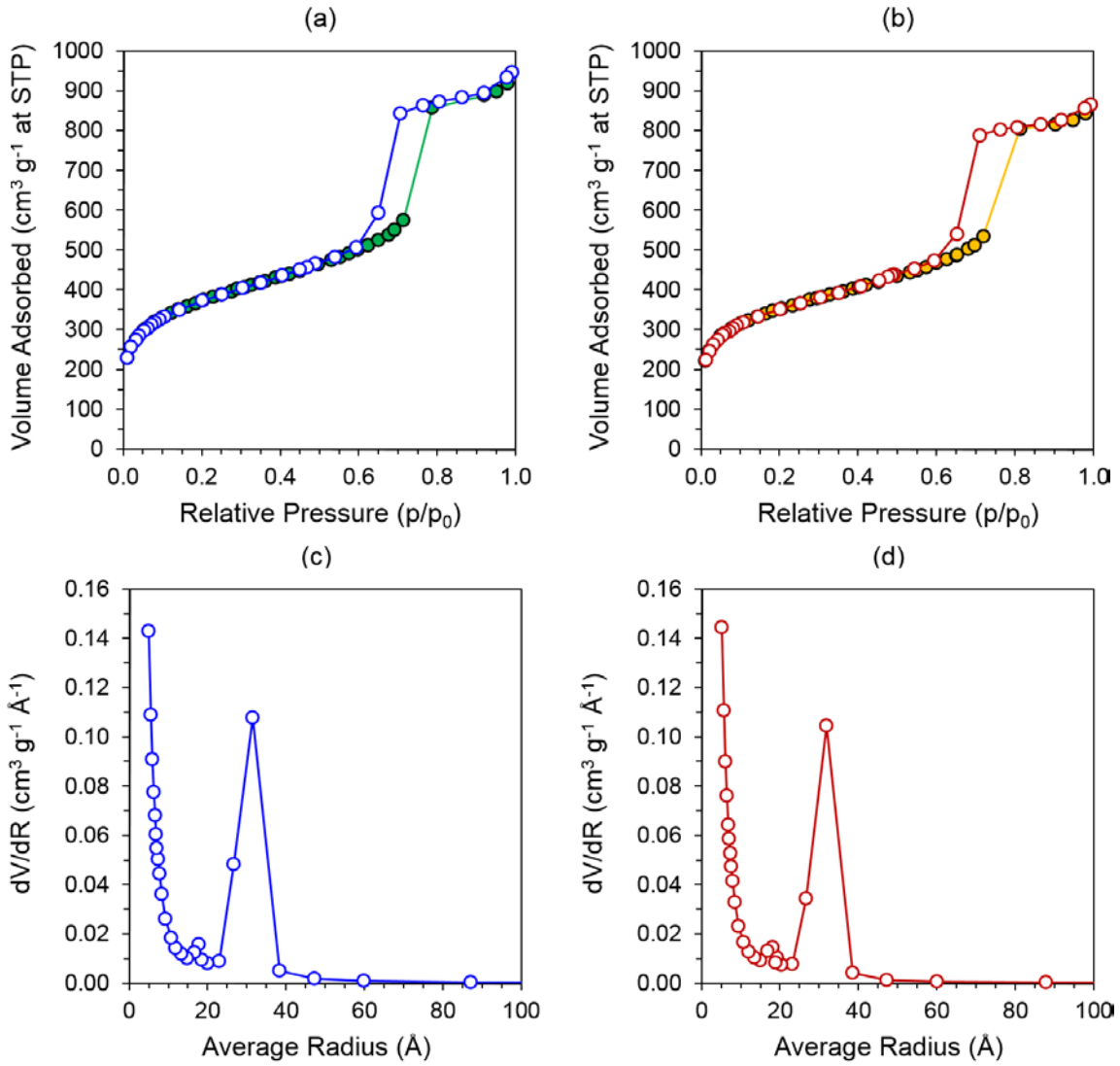

Figure S3. Nitrogen physisorption at 77 K for Nb-SBA-15 materials: (a) isotherm for Nb-0.08-SBA-15, with adsorption (green, filled) and desorption (blue, open) profiles; (b) isotherm for Nb-0.10-SBA-15, with adsorption (yellow, filled) and desorption (red, open) profiles; (c) BJH pore size distribution of Nb-0.08-SBA-15 from the isotherm desorption branch in (a); and (d) BJH pore size distribution of Nb-0.10-SBA-15 from the isotherm desorption branch in (b).

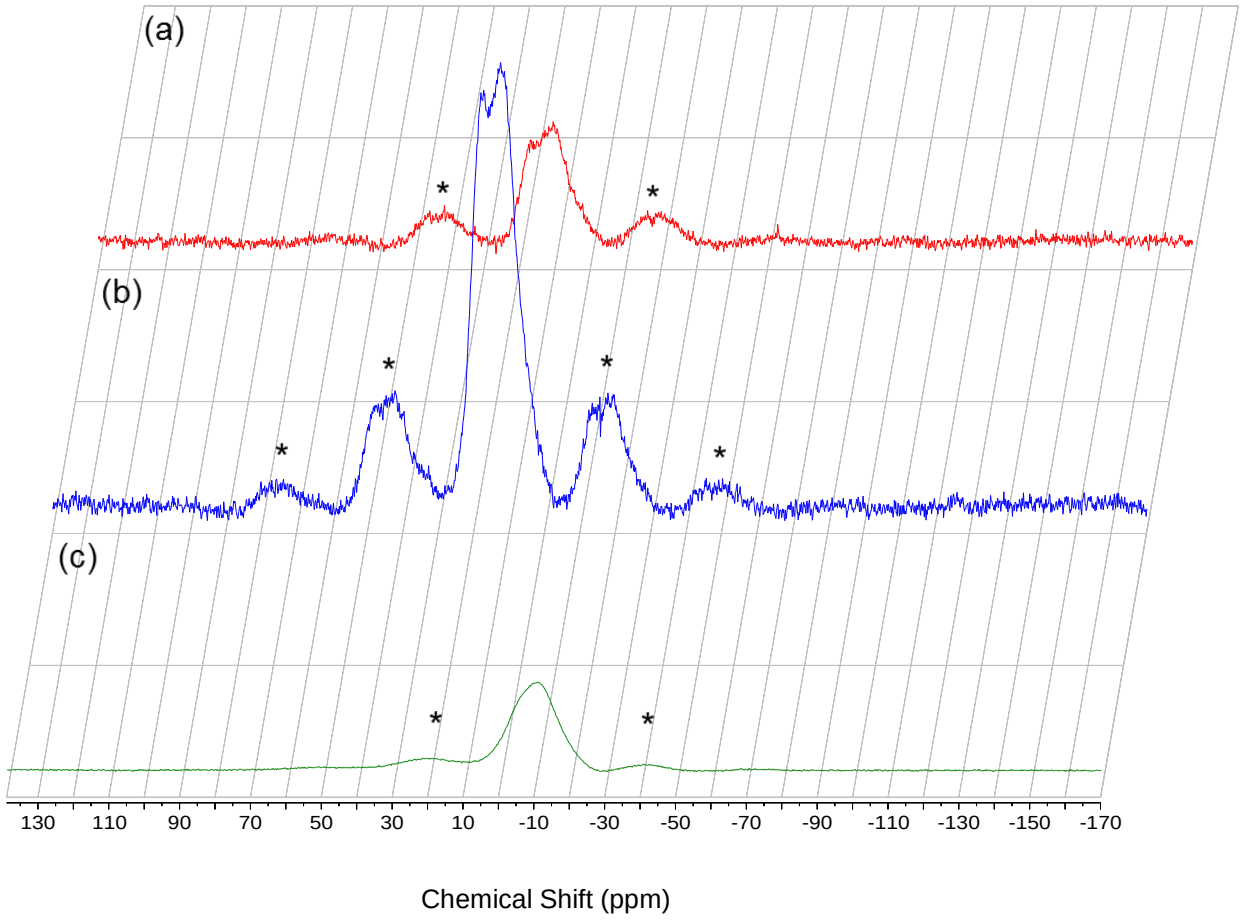

Figure S4. ^{31}P CP-MAS NMR of *in situ* PPA-modified (a) Nb-0.13-Cx and (b) Nb-0.92-Cl, and of (c) bulk niobium phosphate hydrate (as-received, CBMM), collected at a spin rate of 5 kHz. Asterisks denote spinning sidebands. See main text for synthesis conditions.

Table S2. ICP-OES elemental data for ^{31}P CP-MAS NMR materials.

Material	**PPA modification**	**Conc. (mmol g^{-1})**		**P:Nb**
		Nb	**P**	
Nb-0.13-Cx	no	0.13	--	--
	yes	0.13	0.10	0.81
Nb-0.92-Cl	no	0.92	--	--
	yes	0.90	0.14	0.16
bare SiO_2	no	--	0.0	--

Table S3. Experimental kinetic data and model-predicted parameters for the Nb-SiO_2 catalyst series.

Catalyst[a]	Initial Rate[b] (μmol g^{-1} min^{-1})	Rate per total Nb[c] (min^{-1})	*A*, Fraction Active Nb atoms		k_{app}[e] (min^{-1} M^{-1} $(mmol\ Nb)^{-2}$)	Initial TOF[e,f] (min^{-1})
			Graphical[d]	Model[e]		
Nb-0.07-Cx	55.1	0.80	0.58	0.52	5,200	1.5
Nb-0.10-Cx	77.5	0.76	0.52	0.45	6,600	1.7
Nb-0.13-Cx	112	0.88	0.63	0.53	8,600	1.7
Nb-0.20-Cx	192	0.98	0.60	0.60	4,800	1.6
Nb-0.07-Cl	0.92	0.013	0.21	[g]	[g]	[g]
Nb-0.10-Cl	5.6	0.059	0.18	[g]	[g]	[g]
Nb-0.14-Cl	21.6	0.15	0.47	[g]	[g]	[g]
Nb-0.20-Cl	57.0	0.29	0.39	0.21	13,000	1.4
Nb-0.49-Cl	97.3	0.20	0.21	0.15	6,700	1.4
Nb-0.92-Cl	168	0.18	0.25	0.16	2,600	1.1
Nb-1.53-Cl	183	0.12	0.15	0.12	1,800	0.96
Nb-0.23-Cp	162	0.71	0.37	0.39	7,300	1.8
Nb-1.61-Cp	215	0.13	0.18	0.17	1,100	0.81
Nb-0.21-DMA	163	0.79	0.37	0.30	15,000	2.7
Nb-1.57-DMA	215	0.14	0.16	0.11	3,700	1.2
Nb-0.20-OEt	120	0.61	0.39	0.32	11,000	1.9
Nb-0.97-OEt	276	0.28	0.18	0.16	4,100	1.8
Nb-0.08-SBA-15	27.8	0.35	0.62	0.55	2,600	0.64
Nb-0.10-SBA-15	50.8	0.50	0.48	0.42	5,000	1.2
Nb-0.21-Ox-IWI	68.4	0.33	0.25	0.28	6,900	1.2
Nb-0.54-Ox-IWI	46.6	0.086	0.24	0.17	2,000	0.52
Nb-0.20-Cx-C1[h]	35.1	0.18	--	--	--	--
Nb-0.20-Cx-C2[i]	74.9	0.38	--	--	--	--
Nb-0.20-Cx-C3[j]	143.2	0.73	--	--	--	--

[a] Reaction conditions: batch *in situ* PPA poisoning, [*cis*-cyclooctene]$_0$ = 0.11 M, [H_2O_2]$_0$ = 0.35 M, alkene/H_2O_2/Nb/PPA = 140:430:0.7:[0-1.4], V_{tot} = 4.7-4.9 mL. See standard conditions in main article.
[b] Computed for the first 15 minutes of reaction from linear regression fits through product concentration vs. time plots. See Figure 6a.
[c] Initial rate = $mmol_{epoxide}$ $mmol_{total\ Nb}^{-1}$ min^{-1}, computed over the first 15 minutes of experimental reaction data.
[d] Estimated from 95% disappearance of initial rate from log-linear plot of rate vs. added PPA. See Figure 7a and Discussion section of main text for graphical method of estimating *A*.
[e] Estimated from model described by Eq. 11 above. See Section 3.3 of main article and discussion above for details.
[f] Initial intrinsic TOF = $mmol_{epoxide}$ $mmol_{active\ Nb}^{-1}$ min^{-1}, where $mmol_{active\ Nb}$ = $mmol_{total\ Nb}$**A*. Values of *A* determined from model fits.
[g] Catalyst excluded from fit due to insufficient data points (e.g. very low rates) at sub-stoichiometric values of added PPA.
[h] Control trials with constant water concentration at [H_2O] = 3.3 M and variable [PPA] = 0-2.5 mM delivered from a 50 mM solution.
[i] Control trials with constant water concentration at [H_2O] = 1.1 M and variable [PPA] = 0-2.5 mM delivered from a 250 mM solution.
[j] Control trials with variable water concentration [H_2O] = 0.59-3.3 M and constant [PPA] = 0 mM.

Table S4. Physicochemical summary of Group 4 and Group 5 grafted catalysts.

Catalyst	Metal Content[a]			Optical Edge[c] (eV)	Initial Rate[d] (μmol g^{-1} min^{-1})	Fraction active metal[e]
	mmol g^{-1}	M nm^{-2}[b]	wt%			
Ti-0.20-mmCx	0.20	0.21	0.96	3.8	22.9	0.77
Ti-0.21-Cl	0.21	0.22	1.0	3.5	10.6	0.50
Zr-0.23-dmCx	0.23	0.24	2.1	3.6	3.6	0.75
Zr-0.21-Cl	0.21	0.22	1.9	3.0	3.7	0.51
Hf-0.20-dmCx	0.20	0.21	3.6	4.2	11.4	0.76
Hf-0.19-Cl	0.19	0.20	3.3	3.0	1.1	0.30
Nb-0.20-Cx	0.20	0.21	1.8	4.0	192	0.60
Nb-0.20-Cl	0.20	0.21	1.8	3.6	57.0	0.39
Ta-0.22-Cx	0.22	0.23	4.0	3.4[f], 4.5	170	0.60
Ta-0.22-Cl	0.22	0.23	4.0	4.3	28.5	0.51

[a] From ICP-OES of catalysts calcined at 550°C for 6 h.
[b] Using the SiO_2 support BET specific surface area of 570 m^2 g^{-1}. Note that for this SiO_2 support, values of mmol **M** g^{-1} and **M** groups nm^{-2} are nearly equivalent.
[c] Determined from *x*-intercept of the indirect Tauc plot $[F(R)\cdot hv]^{1/2}$ vs. hv (eV), where $F(R)$ is Kubelka-Munk pseudoabsorbance.[6-9]
[d] Computed for the first 15 minutes of reaction from linear regression fits through product concentration vs. time plots. See Figure 6a.
[e] Estimated from 95% disappearance of initial rate from log-linear plot of rate vs. added PPA. See Figure 7a and Discussion section of main text for graphical method of estimating *A*.
[f] Shoulder feature. See Figure S5e.

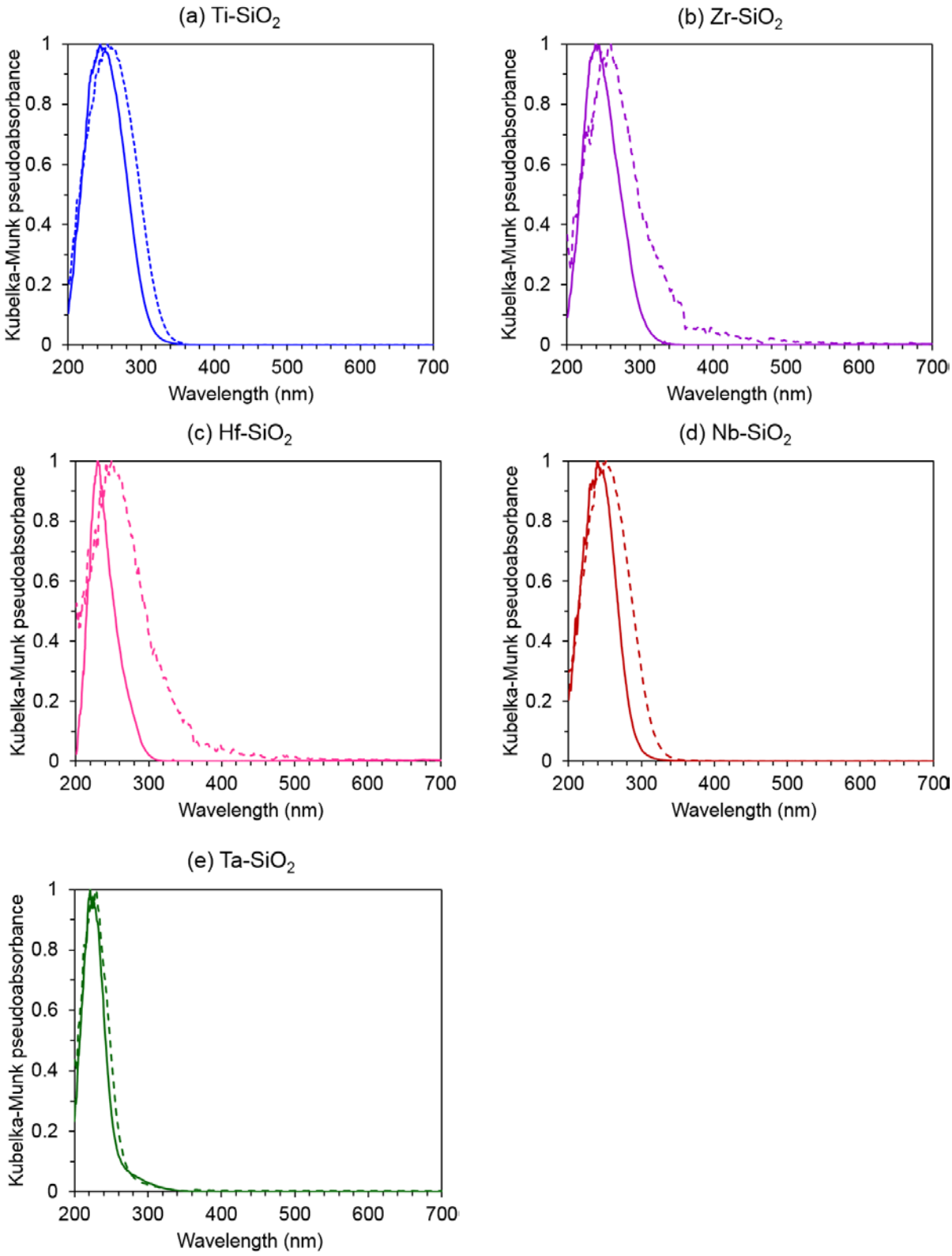

Figure S5. Diffuse reflectance UV-visible spectra of calcined **M**-SiO_2 (**M** = (a) Ti, (b) Zr, (c) Hf, (d) Nb, (e) Ta), from metal-calixarene (solid lines) and metal chloride (dashed lines) precursors. Spectra normalized to sole intense feature.

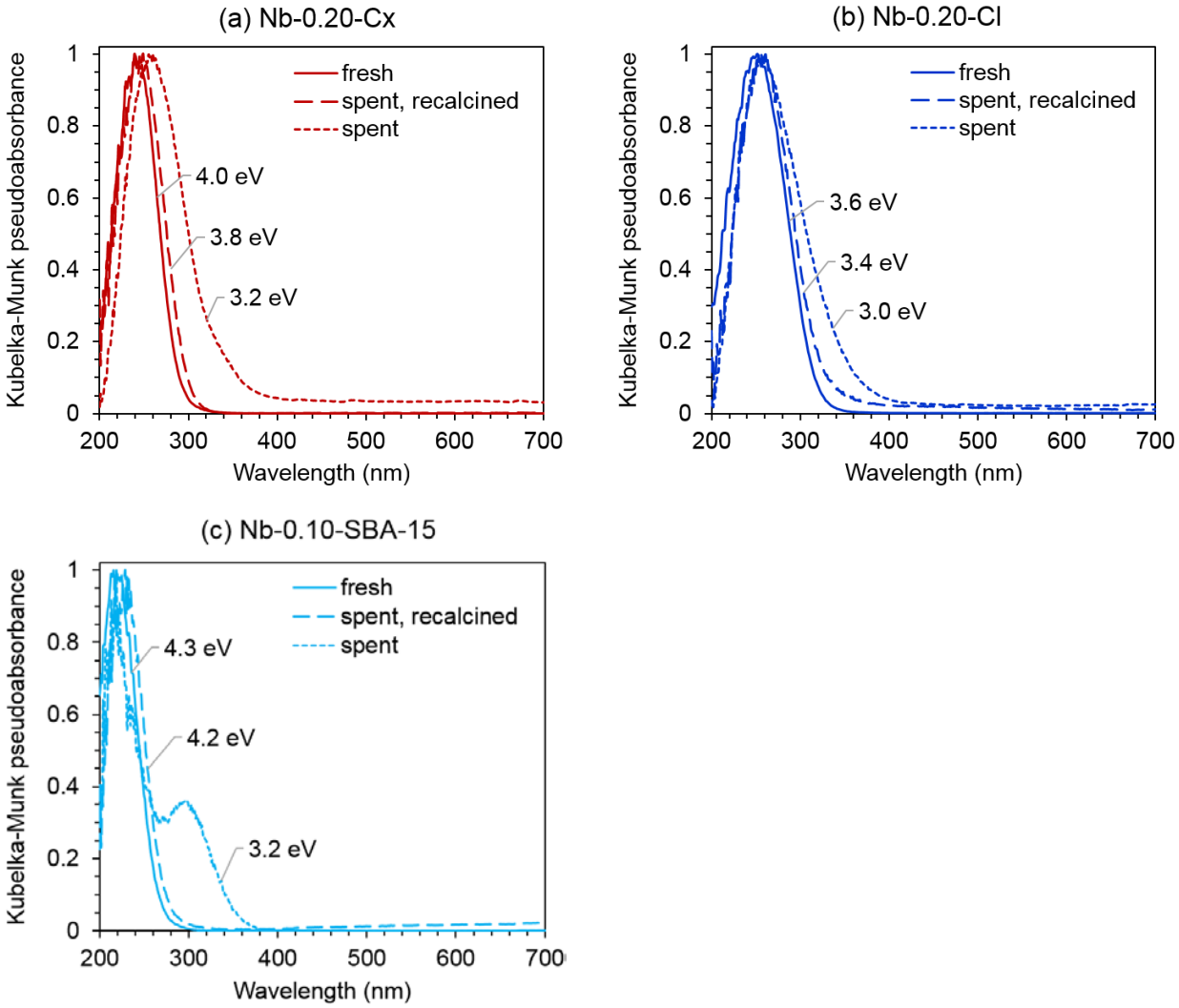

Figure S6. Diffuse reflectance UV-visible spectra of fresh and spent Nb-containing catalysts (a) Nb-0.20-Cx, (b) Nb-0.20-Cl, and (c) Nb-0.10-SBA-15. Fresh catalysts (solid lines) were calcined at 550°C for 6 h in air at a ramp rate of 10 °C min^{-1}. Spent catalysts (short dashed lines) were recovered after 1 h reaction of fresh catlaysts with *cis*-cyclooctene and H_2O_2 under standard conditions at 65°C and washed with acetonitrile. Some spent materials were then recalcined (long dashed lines). Spectra are normalized to the sole intense feature. Labels are optical edge energies from a separate Tauc plot.

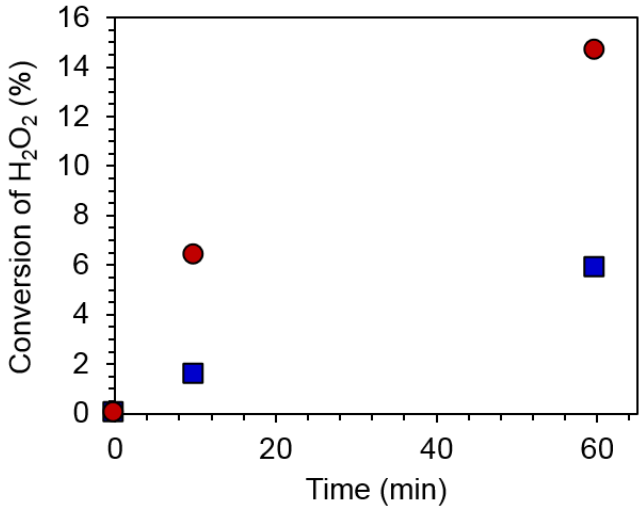

Figure S7. H_2O_2 conversion (%) via disproportionation over Nb-0.20-Cx (red circles) and Nb-0.20-Cl (blue squares) in CD_3CN without alkene at 65°C. Conversion determined via ^{1}H-NMR (16 scans, 500 MHz) using benzene as an internal standard. See reaction conditions in main text. We note that the sustained H_2O_2 decomposition rate at longer times for Nb-0.20-Cx is somewhat larger than that of Nb-0.20-Cl, but not as larger as the difference for initial rate timescales.

Table S5. Average initial H_2O_2 disproportionation rates over Nb-0.20-Cx and Nb-0.20-Cl in CD_3CN at 65°C over the first 10 minutes of reaction. Initial epoxidation rates over the first 15 minutes of reaction under standard kinetic conditions are listed for comparison. See main text for details.

Catalyst	**Init. Rate of H_2O_2 Decomposition (μmol g^{-1} min^{-1})**	**Init. Rate of Epoxidation (μmol g^{-1} min^{-1})**	$r_{0,H2O2\text{-}d}$ / $r_{0,epox}$
Nb-0.20-Cx	350	192	1.8
Nb-0.20-Cl	86	57	1.5
$r_{0,Cx}$ / $r_{0,Cl}$	4.1	3.4	

References

1. Kilos, B.; Nowak, I.; Ziolek, M.; Tuel, A.; Volta, J. C., Transition metal containing (Nb, V, Mo) SBA-15 molecular sieves —synthesis, characteristic and catalytic activity in gas and liquid phase oxidation. In *Stud. Surf. Sci. Catal.*, J. Čejka, N. Ž.; Nachtigall, P., Eds. Elsevier: 2005; Vol. 158, Part B, pp 1461-1468.
2. Trejda, M.; Tuel, A.; Kujawa, J.; Kilos, B.; Ziolek, M., *Microporous Mesoporous Mater.* **2008,** *110*, 271-278.
3. Thornburg, N. E.; Thompson, A. B.; Notestein, J. M., *ACS Catal.* **2015,** *5*, 5077-5088.
4. Lapina, O. B.; Khabibulin, D. F.; Romanenko, K. V.; Gan, Z.; Zuev, M. G.; Krasil'nikov, V. N.; Fedorov, V. E., *Solid State Nucl. Magn. Reson.* **2005,** *28*, 204-224.
5. Cummings, J. P.; Simonsen, S. F., *Am. Mineral.* **1970,** *55*, 90-97.
6. Gao, X.; Bare, S. R.; Fierro, J. L. G.; Banares, M. A.; Wachs, I. E., *J. Phys. Chem. B* **1998,** *102*, 5653-5666.
7. Barton, D. G.; Shtein, M.; Wilson, R. D.; Soled, S. L.; Iglesia, E., *J. Phys. Chem. B* **1999,** *103*, 630-640.
8. Argyle, M. D.; Chen, K.; Resini, C.; Krebs, C.; Bell, A. T.; Iglesia, E., *J. Phys. Chem. B* **2004,** *108*, 2345-2353.
9. Tauc, J.; Menth, A., *J. Non-Cryst. Solids* **1972,** *8–10*, 569-585.